Nociceptive responses in melatonin MT2 receptor knockout mice compared to MT1 and double MT1/MT2 receptor knockout mice

Running Head: MT_2 and mu opioid receptors in neuropathic pain

Supraspinal melatonin MT_2 receptor agonism alleviates pain by interacting with mu opioid receptors

Luca Posa[1,2], Danilo De Gregorio[1,3], Qianzi He [1], Martha Lopez-Canul[1], Emmanuel Darcq[4], Laura Rullo[5], Leora Pearl-Dowler[1], Livio Luongo[6], Sanzio Candeletti[5], Brigitte Lina Kieffer[4], Gabriella Gobbi[1,2,*]

[1] Neurobiological Psychiatry Unit, Department of Psychiatry, McGill University Health Center, McGill University, Montreal, QC, Canada

[2] Alan Edwards Centre for Research on Pain, McGill University, Montreal, QC, Canada

[3] Division of Neuroscience, Vita-Salute San Raffaele University, Milano, Italy

[4] Department of Psychiatry, School of Medicine, Douglas Hospital Research Center, McGill University, Montreal, QC, Canada

[5] Department of Pharmacy and Biotechnology (FaBiT), Alma Mater Studiorum - University of Bologna, Bologna, Italy.

[6] Department of Experimental Medicine, University of Campania "Luigi Vanvitelli", Naples, Italy

***Correspondence to be directed to:**
Gabriella Gobbi, MD, PhD
Neurobiological Psychiatry Unit
Dept. of Psychiatry
McGill University
1033 Pine Avenue West
Montreal, Q.C. Canada H3A 1A1
Email: gabriella.gobbi@mcgill.ca;
Phone: 514-398-1290; Fax: 514-398-4866

Keywords: melatonin, MT_2 receptor, neuropathic pain, opioid, MOR

ABSTRACT

Melatonin through its G protein-coupled MT_2 receptor is implicated in analgesia, but the relationship between MT_2 receptors and the opioid system remains elusive. In neuropathic rodents, the selective melatonin MT_2 agonist UCM924 produced antiallodynia, which was nullified by the pharmacological blockade or genetic inactivation of the mu opioid receptor (MOR), but not the delta opioid receptor (DOR). Indeed MOR, but not neuropathic DOR knockout mice did not respond to the antiallodynic effects of the UCM924. Similarly, the non-selective opioid antagonist naloxone and the selective MOR antagonist CTOP blocked the effects of UCM924 in neuropathic rats, but not the DOR antagonist naltrindole. Electrophysiological recordings in the rostral-ventromedial medulla (RVM) of rats revealed that the typical reduction of the firing activity of pronociceptive ON-cells, and the enhancement of the firing of the antinociceptive OFF-cells, induced by the microinjection of the MT_2 agonist UCM924 into the ventrolateral periaqueductal gray (vlPAG) were blocked by MOR, but not DOR, antagonism. Immunohistochemistry studies showed that MT_2 receptors are expressed in both excitatory ($CaMKII\alpha^+$) and inhibitory ($GAD65^+$) neuronal cell bodies in the vlPAG (~2.16% total), but not RVM. Only 0.20% of vlPAG neurons co-expressed MOR and MT_2 receptors. Collectively, the melatonin MT_2 receptor agonism requires MORs for its antiallodynic effects, mostly through an inter-neuronal interaction between MOR and MT_2 receptors.

1. Introduction

Melatonin is a neurohormone that binds two GPCRs, MT_1 and MT_2, widely expressed in mammalian brains. Clinical studies have shown that melatonin displays analgesic properties in chronic conditions including low back pain, fibromyalgia and migraine[1]. A plethora of animal studies has demonstrated that the effect of melatonin in chronic neuropathic and inflammatory conditions[2] is mediated by the MT_2 receptor[3-6], since its analgesic effects are prevented by the pretreatment with selective MT_2 antagonist 4P-PDOT[4,6,7]. MT_2 receptors are expressed in the ventro-lateral periaqueductal gray (vlPAG)[6,8], an area of the brainstem descending antinociceptive pathways projecting to the rostral-ventromedial medulla (RVM), which in turn projects to the spinal cord[9], a network involved in chronic pain states and in opioid-induced analgesia[9,10]. The selective melatonin MT_2 partial agonist N-{2-([3-bromophenyl]-4-fluorophenylamino)ethyl}acetamide UCM924 shows antiallodynic properties in neuropathic pain models by modulating the ON and OFF neurons of the RVM[6], similarly to other classes of analgesic drugs acting at the central level, including opiates[11]. Although some studies suggest that melatonin's analgesic effects can be blocked by naloxone[12,13], it is still unknown whether the analgesic mechanism of MT_2 receptor agonists is directly or indirectly mediated by opioids. In this study we investigate: 1) the interaction between MT_2 and mu (MOR) or delta (DOR) opioid receptors using a genetic and pharmacological approach; 2) the interaction between MORs and MT_2 receptors in the ON and OFF neurons in the antinociceptive PAG-RVM pathway using *in-vivo* electrophysiology; 3) the cellular localization of MORs and MT_2 receptors at the level of PAG-RVM pathway.

2. Materials and methods

2.1 Animals and animal care

Male Sprague Dawley rats (Charles River, Canada, 140-160 g), male mice lacking mu ($MOR^{-/-}$)[14], or delta ($DOR^{-/-}$)[15] opioid receptors and their wild type littermates (WT) were used for pain behavioural studies and/or for electrophysiological recordings. Male MOR-mCherry knock-in mice expressing the mu opioid receptor fused at its C-terminus to the red protein mCherry were generated by homologous recombination[16], as well as male CaMKIIα-[17,18] and GAD65-tdTomato[19] expressing the red fluorescent tdTomato protein. All the transgenic mice were 20-25 g, PND 5-8 weeks. All animals were housed in standardized animal facilities under a 12-hour light/dark cycle (light on at 7 AM) with ad libitum access to food and water. All the experiments were conducted between 9:00 and 18:00 hours.

Experimental protocols were approved by the Animal Ethics Committees of McGill University (protocol #7181) and followed ethical guidelines of IASP and the Canadian Institutes of Health Research guidelines. All experiments were conducted by experimenters who were blind to drug treatments.

2.2 Pain Animal models

Spared nerve injury was performed according to the method of Decosterd and Woolf[20]. Under isoflurane anesthesia, the sciatic nerve was exposed, the 3 peripheral branches (sural, common peroneal, and tibial nerves) and both tibial and common peroneal nerves were ligated and transected together. Animals recovered for 14 days at the time point of maximal mechanical/thermal allodynia. Mechanical and cold allodynia were absent in healthy (pre-surgery) animals, and the mechanical or thermal withdrawal threshold in rodents before SNI (pre-surgery) was very close to the set cut-offs.

Mechanical allodynia

On day 15 after surgery, animals were placed in a test chamber (elevated mesh platform in an enclosure) separated by opaque dividers and allowed to acclimatize for 30-40 minutes (rats) or 60-90 min (mice). Von Frey filaments (Stoelting, IL) were used to measure the 50% paw withdrawal threshold using the up-and-down method reported by Chaplan et al.[21]. A series of calibrated filaments (Stoelting, IL), ranging from 1.65 (0.008 g) to 5.18 (15 g) bending force) were applied to the midplantar surface (sural portion) of the hind paw. Cutoffs were set at 15 g (for rats) and 2 g (for mice). 50% paw withdrawal threshold were calculated using the formula proposed by Dixon et al.[22]. Animals without allodynia were excluded. After the determination of the basal response, allodynia was assessed at 0.5, 1, 2, 3, 4, 5, 6, 7, and 8 hours (for rats) and 1, 2, 3, 4, 5, 6, 7 (for mice) post-administration for each treatment described below.

Cold plantar essay

Cold allodynia was assed as previously described by Brenner et al.[23]. Briefly, mice were aclimatated on 1/4″ thick pyrex borosilicate glass (Corning Inc., NY) in transparent plastic test chamber for 60-90 min. Fresh dry ice was crushed into a fine powder and was packed into a cut top off 3 mL BD syringe. Awake mice were tested by extending the reformed shaped dry ice pellet and pressing it to the glass underneath the hindpaw using a consistent pressure. The mid plantar portion of the injured paw was targeted ensuring that the paw was touching the glass surface. A stopwatch was used to measure the withdrawal latency. Withdrawal was defined as any vertical or horizontal movement of the paw away from the cold glass. An interval of at least 3 minutes was allowed between trials on any single paw to allow enough time to return to a resting state. A least 3 measurements were made per timepoint and the average of the measurements were calculated. Cutoff was set at 20 seconds to avoid any tissue damage.

2.3 Drugs

UCM924 binding affinity

The affinity of MT_2 partial agonist N-{2-([3-bromophenyl]-4-fluorophenylamino)ethyl}acetamide UCM924[24] for the opioid receptors (MOR, DOR, and KOR) was examined by the Safety47 Panel Dose Response following a scale from 0-100 for response agonism, where 100 is the maximal agonistic response (see methodology in https://www.eurofinsdiscoveryservices.com/catalogmanagement/viewItem/Safety47-Panel-Dose-Response-SAFETYscan-DiscoverX/87-1003DR).

Drugs Administration

For subcutaneous (s.c.) and intra-vlPAG single administrations, UCM924 was dissolved in a vehicle (Veh), (70% DMSO and 30% saline for s.c. or 0.05% DMSO in ACSF for intra-vlPAG injections, as previously described[6]). Naloxone, CTOP (D-Phe-Cys-Tyr-D-Trp-Orn-Thr-Pen-Thr-NH2), naltrindole (Cederlane, ON) were dissolved in vehicle solution. A final volume of 0.4 mL in rats and 0.2 mL in mice was injected for s.c. administration and 1 µL was injected for intra-vlPAG administration. All the antagonists were administrated 10 min before UCM924.

2.4 Intra-vlPAG cannulation and microinjection

Neuropathic rats received guide cannulation and intra-vlPAG microinjections. Animals were anesthetized using isoflurane inhalation and mounted into a stereotaxic apparatus. A stainless-steel guide cannula (4 mm below pedestral; 20 gauge; Plastics One, VA) directed toward the vlPAG using coordinates from the atlas of Paxinos[25] (A: 7.8 mm; L: 0.5 mm from bregma and V: 4.5 mm below the dura). The cannula was secured to the skull with dental cement to a stainless-steel screw. Carprofen (10 mg/kg, s.c.) was administrated immediately and for 2 days post-cannulation. Cannulations were performed 7 days post to SNI. Microinjections were performed using a 25-

gauge needle that extended 2 mm beyond the paired guide cannula into the vlPAG. Drugs or Veh were administered using a 5 µl Hamilton syringe in an automated syringe pump (Braintree Scientific Inc., MA) over a period of 60 seconds. The total microinjection volume was 1 µl. The injection cannula was left in position for 2 min. All cannulae positions were double-checked after microinjection of 0.2 µl of pontamine sky blue dye. Rats with microinjection site outside of the vlPAG were excluded.

2.5 In-vivo electrophysiology

In-vivo electrophysiology coupled to mechanical pinch

Electrophysiological recording were performed as previously described in details[6]. Rats were anesthetized with ethyl-urethane 1.2 g/kg, i.p., placed in a stereotaxic apparatus (David Kopf Instruments, CA), and a hole was drilled through the skull according to the coordinates from rat brain atlas of Paxinos and Watson[25] (2.8-3.3 mm caudal and 0.4-0.9 mm lateral to lambda and 8.9-10.7 mm depth from the surface of the brain).

In the RVM, ON-cells were identified based on their burst of activity, and OFF-cells were identified by the firing pause, when a nociceptive mechanical stimulation (hind-paw pinch) was applied.

Extracellular single-unit recordings were performed using single-barreled pulled glass micropipettes (Stoelting, IL) filled with 2% pontamine sky blue dye in 3 M NaCl. The electrode impedance was between 2 to 5 MΩ. Single-unit activity was recorded as large-amplitude action potentials, amplified by an AC Differential MDA-3 amplifier (BAK Electronics, Inc., FL), post amplified and band-pass filtered by a Realistic 10 band frequency equalizer, digitized by a CED 1401 interface system (Cambridge Electronic Design, UK), processed online, and analyzed off-line using Spike2 software version 5.20.

RVM ON and OFF neurons recording

Once a neuron was identified from its background activity, we optimized spike size and included only those neurons with a constant spike configuration and which could clearly be discriminated from activity in the background throughout the experiment.

The spontaneous single-spike activity (Hz) of the neuron was then recorded for at least 5 minutes before Veh injection. The RVM neural activity was expressed as mean±SEM of the spikes/s by averaging the ongoing cell firing recorded 50 seconds before hind paw flick trials (which were performed every 15 minutes). Paw flick–related ON-cell burst was calculated as mean±SEM of the spikes in the 10 s interval starting from the beginning of the increase in cell frequency (which was at least the double of its spontaneous activity). The duration of the OFF-cell pause was expressed as mean±SEM of the time elapsing between the pause onset and the first spike after the hind paw flick. Pontamine sky blue dye was injected iontophoretically passing a constant positive current of 20 μA for 5 minutes through the recording pipette to mark the recording site. Then, brains were collected and subsequent localization of the labeled site was made by cutting 20-μm-thick brain sections with microtome (Leica CM 3050 S); the electrode placement was identified with microscope (Olympus U-TVO.5 × C-3).

2.6 Immunohistochemistry

Tissue preparation and immunohistochemistry

Tissue preparation and immunohistochemistry were performed according to standard protocols[16,26]. Briefly, 30-μm thick brain coronal sections containing the PAG and RVM were collected using a cryostat (CM3050, Leica) incubated in blocking solution (PB 0.1 M, pH 7.4, 0.5 % Triton X100, 10% donkey serum for 2 h at RT). Sections were then incubated for 48 hours at 4 °C in the blocking solution with appropriate primary antibodies: rabbit polyclonal anti MT_2

(Alomone, AMR-032, 1:250), rat monoclonal anti m-cherry (Invitrogen, M11217, 1:1000), mouse monoclonal anti-parvalbumin (PV) (Millipore, MAB1572, 1:10,000). After washing, sections were incubated for 2 hours at RT with appropriate donkey AlexaFluor-conjugated secondary antibodies: anti-rabbit Alexa 488 (Invitrogen, A-21206, 1:800), anti-rat Alexa 594 (Invitrogen, A-21209, 1:800), and anti-mouse Alexa 647 (Invitrogen, A-31571, 1:800). Sections were washed and incubated with Neurotrace 435/455 blue Nissl (Molecular Probes, N214791, 1:100). Slices were mounted on gelatin-coated slides and coverslips added with mounting medium (DPX, Sigma).

Image acquisition

Images of PAG and RVM were collected with a confocal microscope (Carl Zeiss, LSM710). Acquisitions were performed using X20; 0.80 NA dry objective and zoom values ranging from 0.6 to 1.2 were used for high magnification and images were acquired with the LCS (Leica) software. Confocal acquisitions in the sequential mode (single excitation beams: 405, 488, 594 and 647 nm) to avoid potential crosstalk between the different fluorescence emissions were also used to validate double and triple colocalization. Neurons (cells positive for the specific neuronal marker Neurotrace blue Nissl) expressing a given fluorescent marker were counted using Fiji ImageJ software cell counter plugin. Colocalization between the green fluorescence expression (MT_2), the red (MOR-mCherry, CaMKIIα-tdTomato or GAD65-tdTomato) or blue fluorescence (PV) associated with expression of the neuronal marker was determined manually and blindly for each slice using Fiji ImageJ software. Counting was performed in the well-described area of the vlPAG (Bregma: −4.60 mm to −4.72 mm). At least 3 slices from 4 animals were counted.

2.7 Statistical Analysis

Mechanical allodynia time-course and electrophysiological recordings were analyzed by repeated measures or mixed-model two-way ANOVA (after testing for normality distribution and

sphericity). Areas under the curve (AUC) were analyzed by one-way ANOVA. All data are expressed as mean±S.E.M. Statistical values reaching $P<0.05$ were considered significant. Statistical analyses were performed using Graphpad Prism v8.3.1 (GraphPad Software, CA). Tuckey *post hoc* comparisons was used for pair-wise comparisons when interaction was significant.

3. Results

3.1 Binding affinity of UCM924

UCM924 has 300 times more affinity for the MT_2 (pKi=9.27) than the MT_1 (pKi=6.75) receptor[27]. In *in vitro* pharmacological assays, UCM924 (10 μM) did not display any significant binding affinity for the MOR (OPRM1, max response agonist=2.86), DOR (OPRD1, max response agonist=10.04), and KOR (OPRK1, max response agonist=10.11).

3.2 MT_2-mediated antiallodynic effect of UCM924 is nullified in $MOR^{-/-}$ mice, but not in $DOR^{-/-}$ mice

We first determined the contribution of the opioid system to the MT_2-mediated antiallodynic effect in SNI WT, $MOR^{-/-}$ and $DOR^{-/-}$ mice. 14 days post SNI surgery, the mechanical withdrawal threshold measured in the ipsilateral-operated paw was profoundly lower compared to the contralateral one, in WT (Fig.1A). UCM924 produced a significant mechanical antiallodynic effect in WT (interaction: time x treatment, $F_{7,112}=29.31$, $P<0.001$; UCM924 vs Veh at 2-5h $P<0.001$; Fig.1A) and $DOR^{-/-}$ (interaction: $F_{7,98}=37.25$, $P<0.001$; UCM924 vs Veh at 2-5h $P<0.001$; Fig.1B), but not in $MOR^{-/-}$ (interaction: $F_{7,98}=0.80$, $P=0.59$; Fig. 1C) mice across time. These results were confirmed when comparing all three strains in the AUC (treatment x genotype $F_{2,45}=75.55$, $P<0.001$; WT UCM924 vs $MOR^{-/-}$ UCM924 $P<0.001$; Fig.1D). Similar outcome was

found in the cold allodynia test[23]. UCM924 significantly reduced the SNI-induced cold allodynia, measured as thermal response threshold increase, in WT (interaction: $F_{7,98}$=48.06, P<0.001; UCM924 vs Veh at 2-5h P<0.001; Fig.1E) and $DOR^{-/-}$ mice (interaction: $F_{7,98}$=49.72, P<0.001; UCM924 vs Veh at 2-5h P<0.001; Fig.1F), but not in $MOR^{-/-}$ mice (interaction: $F_{7,112}$=2.07, P=0.052; Fig.1G). These results were confirmed when comparing all three strains in the area under the curve (treatment x genotype $F_{2,42}$=78.99, P<0.001; WT UCM924 vs MOR UCM924 P<0.001; Fig.1H).

3.3 MT_2-mediated antiallodynic effect is nullified by MOR, but not by DOR, blockade

Next, we determined the contribution of the opioid system to the MT_2-mediated antiallodynic effect in SNI rats using pharmacological blockade. The mechanical withdrawal threshold measured in the ipsilateral-operated paw was significantly lower compared to the contralateral one 14 days after SNI surgery (Fig.2A). The subcutaneous administration of 20 mg/kg UCM924 reversed the mechanical allodynia in neuropathic animals (Fig.2A-B), as previously demonstrated[6]. We therefore tested whether the non-selective opioid antagonist naloxone, the selective MOR antagonist CTOP and the DOR antagonist naltrindole counteracted UCM924's effect. Systemic administration of naloxone (1 mg/kg) prior to UCM924 nullified the UCM924-induced antiallodynic effect in SNI rats (interaction: $F_{36,252}$=10.50, P<0.001; naloxone+UCM924 vs UCM924 P<0.05 at 1-6 h; Fig.2A), and the AUC analysis confirmed that the UCM924 effect was prevented by naloxone ($F_{3,23}$=28.28, P<0.001; naloxone+UCM924 vs UCM924 P<0.001; Fig.2B). Importantly, low dose of naloxone (1 mg/kg) alone did not affect the paw withdrawal threshold baseline, as previously reported[28,29]. To explore the selective effect of UCM924 in the PAG, UCM924 (10 μg) was injected intra-vlPAG, where it showed an antiallodynic effect

(Fig.2C-I). This across-time effect was nullified in animals pretreated with intra-vlPAG naloxone (interaction:$F_{15,95}$=16.27, P<0.001; naloxone+UCM924 vs UCM924 at 1h P<0.001; AUC: $F_{3,18}$=53.68, P<0.001; naloxone+UCM924 vs UCM924 P<0.001; Fig.2C-D), CTOP (interaction: $F_{15,100}$=18.83, P<0.001; CTOP+UCM924 vs UCM924 at 1h P<0.001; AUC: $F_{3,19}$=12.19, P<0.001; CTOP+UCM924 vs UCM924 P<0.001; Fig.2E-F), and naltrindole (interaction: $F_{15,115}$=14.02, P<0.001; naltrindole+UCM924 vs UCM924 at 1h P<0.001; AUC: $F_{3,22}$=27.89, P<0.001; naltrindole+UCM924 vs UCM924 P=0.005; Fig.2G-H). The *post hoc* comparisons showed a significant increase of the AUC in naltrindole+UCM924 (but not naloxone+UCM924 or CTOP+UCM924) group compared to vehicle (naltrindole+UCM924 vs Veh P=0.005; Fig.2H). The analysis comparing the AUC of the three antagonists together confirmed that while only naloxone and CTOP completely block UCM924 overall effect (naltrindole+UCM924 vs UCM924, P=0.08; Fig.2I).

3.4 Naloxone and CTOP block the activation of ON and OFF neurons induced by the MT_2 partial agonist UCM924

We next explored the relationship between MORs and MT_2 receptors in the modulation of the ON- and OFF-cells[9,30] the two main populations of neurons in the PAG-RVM circuit implicated in pain modulation. ON-cells increase their firing just prior the occurrence of reflexes induced by noxious stimulation, playing a pronociceptive role. OFF-cells undergo a characteristic pause just before the nocifensive reflex, and their activation promotes antinociception[11,31]. In SNI rats the mean frequency of spontaneous activity was 14.5±1.1 spikes/s for ON-cells, and 4.0±0.7 spikes/s for OFF-cells. While microinjection of Veh into the vlPAG did not alter the spontaneous activity of ON- or OFF-cells[6], UCM924 microinjection (Fig.3A-B) decreased the firing rate of the pronociceptive ON-cells (Fig.3C top left, D, F, H) and enhanced that of the antinociceptive OFF-

cells (Fig.3C top right, E, G, I) as previously determined[6]. Intra-vlPAG naloxone pre-treatments abolished the UCM924-induced decrease in the frequency of the spontaneous activity (interaction: $F_{24,91}$=7.73, P<0.001; UCM924 vs naloxone+UCM924 at 25-55 min P<0.001; Fig.3C bottom left, D) and in the mechanical pinch burst of firing (Fig.4A) in the ON-cells. CTOP also abolished the effects of UCM924 (interaction: $F_{24,91}$=6.00, P<0.001; UCM924 vs CTOP+UCM924 at 20-55 min P<0.001; Fig.3F) and in the mechanical pinch burst (Fig.4C) in the ON-cells. Together, naloxone and CTOP prevented the enhanced firing of the OFF-cells (UCM924 vs naloxone+UCM924 interaction: $F_{24,91}$=3.77, P<0.001; UCM924 vs CTOP+UCM924 interaction: $F_{24,91}$=5.62, P<0.001; Fig.3C bottom right, 3E and 3G, respectively) and the reduction of the OFF-cell pause duration (Fig.4D) promoted by UCM924. In agreement with the behavioural data, the naltrindole neither altered the modulation of the ON-OFF firing activity induced by UCM924 (UCM924 vs naltrindole+UCM924 vs at 0-60 min, P=n.s., Fig.3 H-I), nor the burst and pause of ON- and OFF-cells (Fig.4E-F, respectively).

3.5 MT_2 receptors and MORs are expressed in different areas and neurons of the PAG-RVM descending pathway

To explore the neurobiological and anatomical mechanisms underlying the antinociceptive effects in the PAG-RVM circuit, we then investigated the localization of MT_2 receptors using SNI transgenic MOR-mCherry[26], CaMKIIα-tdTomato[18], GAD65-tdTomato mouse[19] and the PV[32-34]. Our previous immunohistochemical results showed that the MT_2 receptor[6,8] and MOR-mCherry[16] are both expressed in the vlPAG. MT_2 receptors have been found in GAD65-tdTomato$^+$ cells of the vlPAG (Fig.5A), and specifically this co-localization was observed in PV-inhibitory interneurons (Fig.5A and C). Using transgenic mice lines CaMKIIα-td tomato, we also confirmed

that MT_2 receptors co-localize with CaMKIIα, an excitatory neuronal promoter in the adult forebrain[17,18] (Fig.5B).

We then quantified the percentage of neurons positive for somatic MT_2 and MOR-mCherry in the vlPAG. While we counted 2.16±0.32% of MT_2^+ in the total neural cell body population of the vlPAG (17/768), 1.19±0.18% of MOR were quantified over the total vlPAG neural population (9/768) (Fig. 5C). The co-localization MT_2^+/MOR-Cherry$^+$ neurons were only 0.20±0.02 % of the total vlPAG neurons (2/768) (Fig.5C). Specifically, among the population of MOR-mCherry$^+$ in the vlPAG 17.14±2.62% co-labeled with MT_2^+ expressing neurons (2/9), and among the MT_2^+ neurons 9.44±4.24% co-labeled with MOR-mCherry$^+$ in the vlPAG (2/16) (Fig.5C).

Moreover, while MOR-mCherry signal was revealed in PV$^+$-inhibitory neuronal cell bodies in the RVM, MT_2 receptor immunoreactivity was instead absent (Fig.5D).

Altogether, these data suggest that MT_2 and MOR are differentially expressed in distinct neuronal populations of the PAG and in distinct brain areas.

4. Discussion

The results presented here showed that the supraspinal antiallodynic effects of the melatonin MT_2 agonist UCM924 are mediated by the opioid system, specifically by MORs.

Our results showed that UCM924, a selective MT_2 partial agonist belonging to the class of N-(substituted-anilinoethyl)amides[27], has no affinity for opioid receptors, in keeping with recent findings showing distinct conformational features between MORs and MT_2 receptors[35].

The antiallodynic effects of MT_2 agonist are blocked by the genetic and pharmacological blockage of MOR, but not DOR. Similarly, the CTOP, but not naltrindole, blocks the ability of UCM924 to

decrease pronociceptive ON-cells firing and burst and increase antinociceptive OFF-cells firing and reduce their pause.

Previous studies have shown that exogenous and endogenous melatonin provides analgesic effects with the involvement of the opioid system. Notably, melatonin increases the release of beta-endorphin[36,37], and naloxone blocks melatonin-induced analgesia in the hot plate[12,38] and tail-flick tests[39]. Furthermore, the opioid antagonist naltrexone blocks melatonin-induced mechano-allodynia in a spinal nerve ligation model[13]. We showed that non-selective naloxone and MOR-selective CTOP antagonists both blocked the antiallodynic effect as well as the central modulation of ON- and OFF-cells in the PAG-RVM descending antinociceptive circuit. On the other hand, we found that naltrindole, at the dose of 1µg intra-PAG showing a selective DOR antagonism *in vivo*[40], had a limited effectiveness in blocking the effect of UCM924, in agreement with a previous observations[3]. This finding was confirmed by the electrophysiological recordings in ON- and OFF-cells (where naltrindole did not block the effects of UCM924) as well as by the mechanical and cold allodynic tests performed in $DOR^{-/-}$ mice with UCM924. Although we cannot completely rule out the role of DOR in neuropathic conditions at peripheral level[41,42], the findings presented here suggest that MOR, but not DOR, is involved in MT_2-promoted supraspinal antiallodynia.

Immunohistochemical data confirm that MT_2 receptors are expressed in neurons of the vlPAG[6,8], but not in the RVM. We found that MT_2 receptors are expressed in both excitatory ($CaMKII\alpha^+$) and inhibitory ($GAD65^+$) neuronal cell bodies in the vlPAG (~2.16% total), while 1.19% of MORs have been found in somatodendritic neuronal population. On the other hand, our findings confirmed that some MORs are expressed in the PAG[43,44] and abundantly in the RVM[45,46], corroborating the hypothesis that MT_2 receptors are localized upstream of MORs in the antinociceptive descending pathway. The presence of MT_2 in vlPAG glutamategic neurons were

also found in our previous work[6], using vGlut2 antibody, even if the GABAergic neurons marked with vGAT resulted non expressing the MT_2 receptors. This discrepancy is likely due to the fact that vGlut2 and vGAT antibodies mark the presence of the receptors at the synaptic terminal level of glutamatergic or GABAergic neurons, respectively. Only a minimal number (~0.2%) of vlPAG neurons co-expressed MOR and MT_2 receptors, suggesting an inter-cellular interaction between these two neuronal populations. Since both MOR and MT_2 receptors belong to GPCRs coupled to a Gαi-dependent cAMP and ERK signalling pathways[47,48], an intra-cellular cross-talk cannot be *a priori* excluded.

A large body of literature suggests that MORs are localized at the somatodendritic level of ON-cell of RVM (receiving inputs from PAG glutamatergic neurons) and at the GABA-realising presynaptic terminal of the OFF neurons[9,30,49]. Indeed, OFF cells are activated by local infusion of either MOR selective ligands or the $GABA_A$ receptor antagonist bicuculline[50,51], and ON-cells activity is depressed by morphine administration in the RVM[52].

The MT_2 receptors localized in the PAG glutamatergic neurons as well as in the GABAergic neurons may control upstream the modulation of MOR acting on ON- and OFF-cells of the RVM (see Fig.6). While the effect promoted by the MT_2 receptor agonism on excitatory neurons in the vlPAG might directly silencing pronociceptive ON-cells, in parallel would disinhibit GABAergic neurons in the vlPAG to modulate the activity of the OFF-cells; altogether, these effects would promote analgesia.

Morphine and other synthetic opiates are the cause of the so-called “opioid crisis” in North-America[53,54] leading to the death of 100 people a day in the US alone[55], consequently the MT_2 receptor agonism may represent a novel avenue to treat chronic neuropathic pain conditions by the indirect engagement of the opioid system.

Funding and disclosure

The research was sponsored by the Canadian Institutes for Health Research (CIHR, MOP-130285), Brain Canada and the Quebec Consortium for Drug Discovery (CQDM) to G.G. L.P. received scholarship from of the The Louise and Alan Edwards Foundation and Fonds Recherche Québec-Santé (FRQS); D.D.G. from FRQS and CIHR, M.L.C from McGill Faculty of Medicine/Ferring. G.G. is an inventor of patents in selective melatonin MT_2 ligands. The remaining authors declare no conflict of interest.

Author Contribution

L.P. designed the study, performed experiments, analyzed data and wrote and edited the main draft of the manuscript. D.D.G. performed preliminary electrophysiological experiments and helped in data analysis. Q.H., E.D. and L.L assisted in immunohistochemical experiments. M.L.C. assisted in behavioural experiments. L.R. and L.P-D. and assisted in experiments and data analysis. S.C. assisted in experimental design. B.L.K. assisted in experimental design and contributed to write the manuscript. G.G. supervised the project, designed experiments, and wrote the manuscript. Authors thank Drs Arkady Khoutorsky and Alfredo Ribeiro-da-Silva for providing CaMKIIα- and GAD65-tdTomato mice.

References

1. Wilhelmsen M, Amirian I, Reiter RJ, Rosenberg J, Gögenur I. Analgesic effects of melatonin: a review of current evidence from experimental and clinical studies. *Journal of pineal research.* 2011;51(3):270-277.
2. Posa L, De Gregorio D, Gobbi G, Comai S. Targeting melatonin MT2 receptors: A novel pharmacological avenue for inflammatory and neuropathic pain. *Current medicinal chemistry.* 2018;25(32):3866-3882.
3. Arreola-Espino R, Urquiza-Marín H, Ambriz-Tututi M, et al. Melatonin reduces formalin-induced nociception and tactile allodynia in diabetic rats. *European journal of pharmacology.* 2007;577(1-3):203-210.
4. Lin TB, Hsieh MC, Lai CY, et al. Melatonin relieves neuropathic allodynia through spinal MT 2-enhanced PP 2Ac and downstream HDAC 4 shuttling-dependent epigenetic modification of hmgb1 transcription. *Journal of pineal research.* 2016;60(3):263-276.
5. Lopez-Canul M, Comai S, Domínguez-López S, Granados-Soto V, Gobbi G. Antinociceptive properties of selective MT2 melatonin receptor partial agonists. *European journal of pharmacology.* 2015;764:424-432.
6. Lopez-Canul M, Palazzo E, Dominguez-Lopez S, et al. Selective melatonin MT2 receptor ligands relieve neuropathic pain through modulation of brainstem descending antinociceptive pathways. *Pain.* 2015;156(2):305-317.
7. Tu Y, Sun R-Q, Willis WD. Effects of intrathecal injections of melatonin analogs on capsaicin-induced secondary mechanical allodynia and hyperalgesia in rats. *Pain.* 2004;109(3):340-350.
8. Lacoste B, Angeloni D, Dominguez-Lopez S, et al. Anatomical and cellular localization of melatonin MT1 and MT2 receptors in the adult rat brain. *Journal of pineal research.* 2015;58(4):397-417.
9. Fields H, Barbaro NM, Heinricher M. Brain stem neuronal circuitry underlying the antinociceptive action of opiates. *Progress in brain research.* 1988;77:245-257.
10. Ossipov MH, Morimura K, Porreca F. Descending pain modulation and chronification of pain. *Current opinion in supportive and palliative care.* 2014;8(2):143-151.
11. Heinricher MM, Morgan MM, Tortorici V, Fields HL. Disinhibition of off-cells and antinociception produced by an opioid action within the rostral ventromedial medulla. *Neuroscience.* 1994;63(1):279-288.
12. Lakin M, Miller C, Stott M, Winters W. Involvement of the pineal gland and melatonin in murine analgesia. *Life Sciences.* 1981;29(24):2543-2551.
13. Ambriz-Tututi M, Granados-Soto V. Oral and spinal melatonin reduces tactile allodynia in rats via activation of MT2 and opioid receptors. *Pain.* 2007;132(3):273-280.
14. Matthes HW, Maldonado R, Simonin F, Valverde O. Loss of morphine-induced analgesia, reward effect and withdrawal symptoms in mice lacking the mu-opioid-receptor gene. *Nature.* 1996;383(6603):819.
15. Filliol D, Ghozland S, Chluba J, et al. Mice deficient for δ-and μ-opioid receptors exhibit opposing alterations of emotional responses. *Nature genetics.* 2000;25(2):195-200.
16. Erbs E, Faget L, Scherrer G, et al. A mu–delta opioid receptor brain atlas reveals neuronal co-occurrence in subcortical networks. *Brain Structure and Function.* 2015;220(2):677-702.
17. Dragatsis I, Zeitlin S. CaMKIIα-cre transgene expression and recombination patterns in the mouse brain. *Genesis.* 2000;26(2):133-135.

18. Tsien JZ, Chen DF, Gerber D, et al. Subregion-and cell type–restricted gene knockout in mouse brain. *Cell.* 1996;87(7):1317-1326.
19. Besser S, Sicker M, Marx G, et al. A transgenic mouse line expressing the red fluorescent protein tdTomato in GABAergic neurons. *PLoS One.* 2015;10(6):e0129934.
20. Decosterd I, Woolf CJ. Spared nerve injury: an animal model of persistent peripheral neuropathic pain. *Pain.* 2000;87(2):149-158.
21. Chaplan S, Bach F, Pogrel J, Chung J, Yaksh T. Quantitative assessment of tactile allodynia in the rat paw. *Journal of neuroscience methods.* 1994;53(1):55-63.
22. Dixon WJ. Efficient analysis of experimental observations. *Annual review of pharmacology and toxicology.* 1980;20(1):441-462.
23. Brenner DS, Golden JP, Gereau IV RW. A novel behavioral assay for measuring cold sensation in mice. *PloS one.* 2012;7(6):e39765.
24. Rivara S, Lodola A, Mor M, et al. N-(substituted-anilinoethyl) amides: design, synthesis, and pharmacological characterization of a new class of melatonin receptor ligands. *Journal of medicinal chemistry.* 2007;50(26):6618-6626.
25. Paxinos G, Watson C. *The Rat Brain in stereotaxic coordinates 7th Edition.* New York: Academic Press; 2013.
26. Erbs E, Faget L, Veinante P, Kieffer BL, Massotte D. In vivo neuronal co-expression of mu and delta opioid receptors uncovers new therapeutic perspectives. *Receptors & clinical investigation.* 2014;1(5):210.
27. Rivara S, Vacondio F, Fioni A, et al. N-(Anilinoethyl) amides: Design and Synthesis of Metabolically Stable, Selective Melatonin Receptor Ligands. *ChemMedChem: Chemistry Enabling Drug Discovery.* 2009;4(10):1746-1755.
28. Kocher L. Systemic naloxone does not affect pain-related behaviour in the formalin test in rat. *Physiology & behavior.* 1988;43(3):265-268.
29. Posa L, Lopez-Canul M, Rullo L, et al. Nociceptive responses in MT2 receptor knockout mice compared to MT1 and double MT1/MT2 receptor knockout mice. *Journal of Pineal Research.* 2020;69:e12671.
30. Fields H. State-dependent opioid control of pain. *Nature Reviews Neuroscience.* 2004;5(7):565-575.
31. Fields HL, Heinricher MM, Mason P. Neurotransmitters in nociceptive modulatory circuits. *Annual review of neuroscience.* 1991;14(1):219-245.
32. Barbaresi P, Mensà E, Lariccia V, Pugnaloni A, Amoroso S, Fabri M. Differential distribution of parvalbumin-and calbindin-D28K-immunoreactive neurons in the rat periaqueductal gray matter and their colocalization with enzymes producing nitric oxide. *Brain Research Bulletin.* 2013;99:48-62.
33. Celio M. Calbindin D-28k and parvalbumin in the rat nervous system. *Neuroscience.* 1990;35(2):375-475.
34. Fukuda T, Heizmann CW, Kosaka T. Quantitative analysis of GAD65 and GAD67 immunoreactivities in somata of GABAergic neurons in the mouse hippocampus proper (CA1 and CA3 regions), with special reference to parvalbumin-containing neurons. *Brain research.* 1997;764(1-2):237-243.
35. Wang Q, Lu Q, Guo Q, et al. Structural basis of the ligand binding and signaling mechanism of melatonin receptors. *Nature Communications.* 2022;13(1):1-10.
36. Barrett T, Kent S, Voudouris N. Does melatonin modulate beta-endorphin, corticosterone, and pain threshold? *Life sciences.* 2000;66(6):467-476.

37. Shavali S, Ho B, Govitrapong P, et al. Melatonin exerts its analgesic actions not by binding to opioid receptor subtypes but by increasing the release of β-endorphin an endogenous opioid. *Brain research bulletin.* 2005;64(6):471-479.
38. Golombek DA, Escolar E, Burin LJ, Sánchez MGDB, Cardinali DP. Time-dependent melatonin analgesia in mice: inhibition by opiate or benzodiazepine antagonism. *European journal of pharmacology.* 1991;194(1):25-30.
39. Wang T, Li S-r, Dai X, Peng Y-l, Chen Q, Wang R. Effects of melatonin on orphanin FQ/nociceptin-induced hyperalgesia in mice. *Brain research.* 2006;1085(1):43-48.
40. Calcagnetti DJ, Holtzman SG. Delta opioid antagonist, naltrindole, selectively blocks analgesia induced by DPDPE but not DAGO or morphine. *Pharmacology Biochemistry and Behavior.* 1991;38(1):185-190.
41. Holdridge SV, Cahill CM. Spinal administration of a δ opioid receptor agonist attenuates hyperalgesia and allodynia in a rat model of neuropathic pain. *European Journal of Pain.* 2007;11(6):685-693.
42. Kabli N, Cahill CM. Anti-allodynic effects of peripheral delta opioid receptors in neuropathic pain. *Pain.* 2007;127(1-2):84-93.
43. Vaughan C, Ingram S, Connor M, Christie M. How opioids inhibit GABA-mediated neurotransmission. *Nature.* 1997;390(6660):611-614.
44. Commons KG, Van Bockstaele EJ, Pfaff DW. Frequent colocalization of mu opioid and NMDA-type glutamate receptors at postsynaptic sites in periaqueductal gray neurons. *Journal of Comparative Neurology.* 1999;408(4):549-559.
45. Zhang W, Gardell S, Zhang D, et al. Neuropathic pain is maintained by brainstem neurons co-expressing opioid and cholecystokinin receptors. *Brain.* 2009;132(3):778-787.
46. Marinelli S, Vaughan CW, Schnell SA, Wessendorf MW, Christie MJ. Rostral ventromedial medulla neurons that project to the spinal cord express multiple opioid receptor phenotypes. *Journal of Neuroscience.* 2002;22(24):10847-10855.
47. Al-Hasani R, Bruchas MR. Molecular mechanisms of opioid receptor-dependent signaling and behavior. *Anesthesiology: The Journal of the American Society of Anesthesiologists.* 2011;115(6):1363-1381.
48. Cecon E, Oishi A, Jockers R. Melatonin receptors: molecular pharmacology and signalling in the context of system bias. *British journal of pharmacology.* 2018;175(16):3263-3280.
49. Heinricher MM, Fields HL. Central nervous system mechanisms of pain modulation. In: Elsevier, ed. *Wall & Melzack's Textbook of Pain.* 6th ed. London2013:129-142.
50. Finnegan TF, Li D-P, Chen S-R, Pan H-L. Activation of μ-opioid receptors inhibits synaptic inputs to spinally projecting rostral ventromedial medulla neurons. *Journal of Pharmacology and Experimental Therapeutics.* 2004;309(2):476-483.
51. Heinricher M, Tortorici V. Interference with GABA transmission in the rostral ventromedial medulla: disinhibition of off-cells as a central mechanism in nociceptive modulation. *Neuroscience.* 1994;63(2):533-546.
52. Heinricher M, Morgan M, Fields H. Direct and indirect actions of morphine on medullary neurons that modulate nociception. *Neuroscience.* 1992;48(3):533-543.
53. Fischer B, Pang M, Tyndall M. The opioid death crisis in Canada: crucial lessons for public health. *The Lancet Public Health.* 2019;4(2):e81-e82.

54. Hoots BE, Xu L, Kariisa M, et al. 2018 Annual surveillance report of drug-related risks and outcomes - United States. 2018.
55. CDC/NCHS. National Vital Statistics System, Mortality. In: US Department of Health and Human Services C, ed. Atlanta, GA: CDC WONDER; 2018.

Figure legends

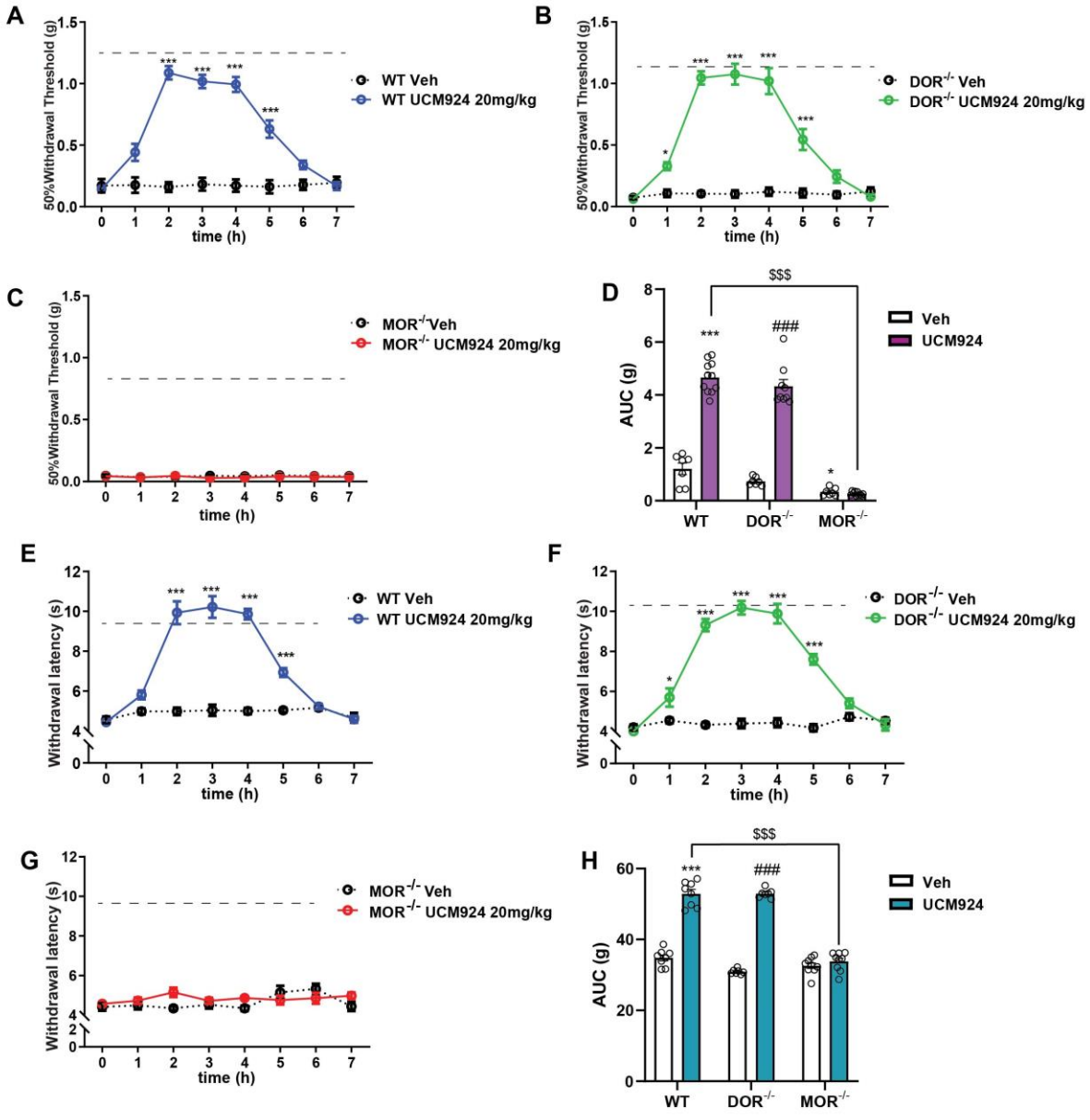

Figure 1. The MT_2 agonist UCM924 does not have anti-allodynic effect in MOR knockout mice. Mechanical allodynia test. UCM924 (20 mg/kg, s.c.) increases the paw withdrawal threshold across time in WT (**A**) and $DOR^{-/-}$ (**B**), but not in $MOR^{-/-}$ (**C**) neuropathic mice. (**D**) Area under the curve (AUC): UCM924 (20 mg/kg, s.c.) produces an overall antiallodynic effect in WT and $DOR^{-/-}$, but not in $MOR^{-/-}$, neuropathic mice. Data are expressed as mean ± SEM (n= 11-7 each group). Thermal allodynia test. UCM924 (20 mg/kg, s.c.) increases the paw withdrawal

latency in WT (**E**) and DOR$^{-/-}$ (**F**), but not in MOR$^{-/-}$ (**G**), neuropathic mice. (**H**) AUC: UCM924 (20 mg/kg, s.c.) produces a cumulative antiallodynic effect in WT and DOR$^{-/-}$, but not in MOR$^{-/-}$, neuropathic mice. Data are expressed as mean ± SEM (n= 9-7 each group). Intermittent line on the top represents the mechanical or latency withdrawal threshold of the contralateral paw. *P < 0.05, and ***P < 0.001 vs WT Veh (**A, E**) or DOR$^{-/-}$ Veh (**B, F**); ###P < 0.001 vs DOR$^{-/-}$ Veh (**D, H**), $$$ < 0.001 vs WT UCM924 (**D, H**). Data are analyzed using two-way ANOVA followed by Tukey post-hoc test.

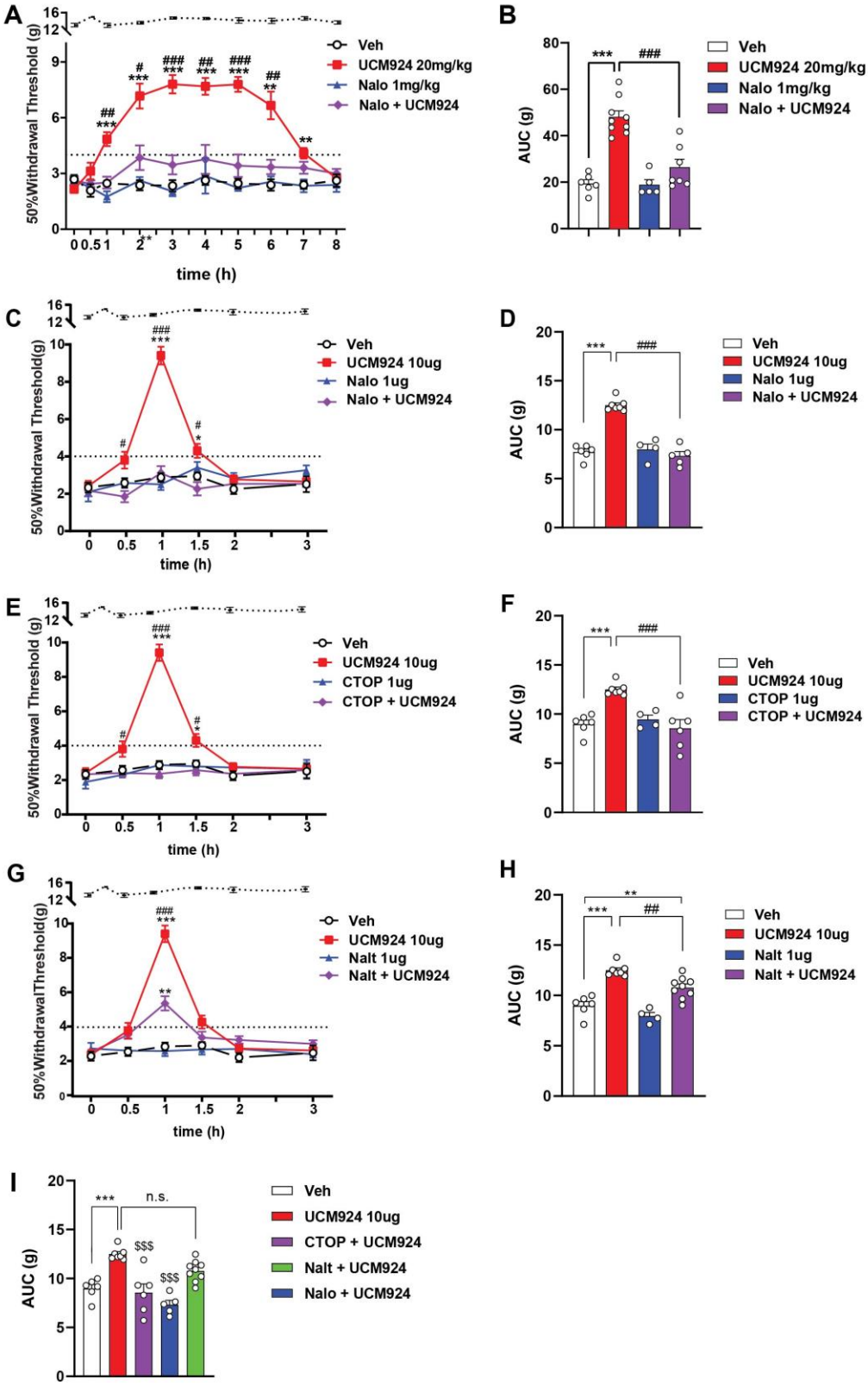
A
50%Withdrawal Threshold (g)
time (h)
Veh
UCM924 20mg/kg
Nalo 1mg/kg
Nalo + UCM924
B
AUC (g)
C
50%Withdrawal Threshold(g)
UCM924 10ug
Nalo 1ug
D
E
CTOP 1ug
CTOP + UCM924
F
G
Nalt 1ug
Nalt + UCM924
H
I
n.s.

Figure 2. The antiallodynic effect of the MT_2 agonist UCM924 is nullified by the non-selective naloxone and selective MOR antagonist CTOP. (A) Time course. UCM924 (20 mg/kg, s.c.) increases the paw withdrawal threshold in neuropathic rats. Pretreatment with the non-selective opioid antagonist naloxone (1 mg/kg, s.c.) blocks the UCM924 antiallodynic effect across time. **(B)** AUC: UCM924 (20 mg/kg, s.c.) produces a significant antiallodynic effect for 7 hours. Pretreatment with naloxone (1 mg/kg, s.c.) reduces the overall UCM924 antiallodynic effect across time. **(C, E and G)** Time course. UCM924 (10 μg, intra-vlPAG) increases the paw withdrawal threshold in neuropathic rats. Pretreatment with naloxone or MOR selective CTOP (1 μg, intra-vlPAG, both) completely blocks the UCM924 antiallodynic effect. **(D** and **F)** AUC: Pretreatment with naloxone or CTOP (1 μg, intra-vlPAG, both) reduces the overall UCM924 antiallodynic effect. **(G)** Time course. Pretreatment with the selective DOR antagonist naltrindole (1 μg, intra-vlPAG) partially blocks the UCM924 antiallodynic effect at 1 hour. **(H)** AUC: Pretreatment with naltrindole (1 μg, intra-vlPAG) reduces the overall UCM924 antiallodynic effect. Intermittent line on the top represents the mechanical withdrawal threshold of contralateral paw. Intermittent line on the bottom represents the threshold cutoff (4 g) for allodynia in SNI rats. Values above this line are considered an antiallodynic effect. Data are expressed as mean ± SEM (n= 9-4 each group). *P < 0.05, **P < 0.01, and ***P < 0.001 vs Veh; #P < 0.05, ##P < 0.01, and ###P < 0.001 vs naloxone or CTOP or naltrindole + UCM924. Data are analyzed using two-way ANOVA (time course) or one-way ANOVA (AUC) followed by Tukey post-hoc test.

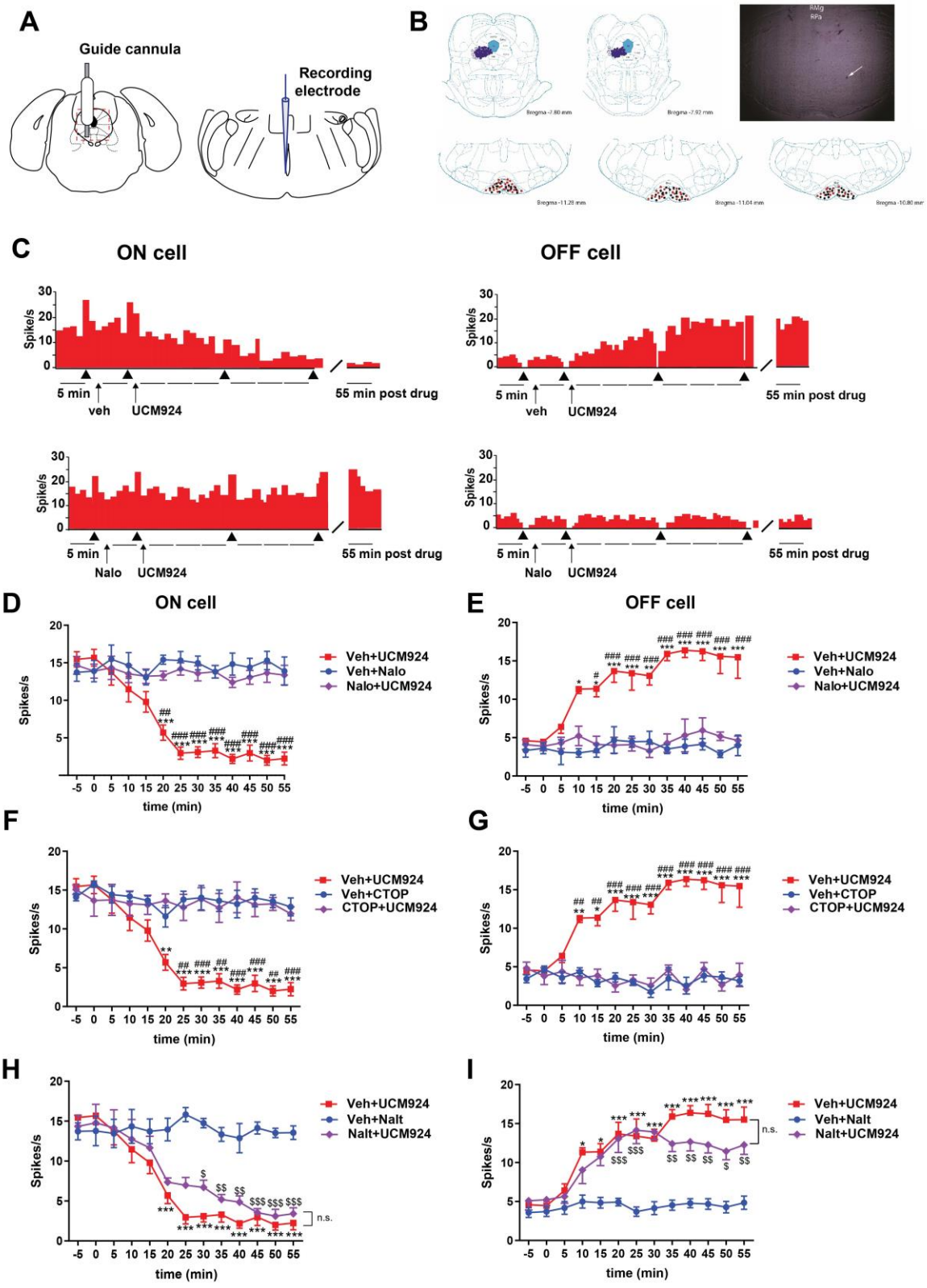
A
Guide cannula
Recording electrode
B
C
ON cell
OFF cell
Spike/s
5 min
veh
UCM924
55 min post drug
Nalo
D
ON cell
E
OFF cell
Spikes/s
time (min)
Veh+UCM924
Veh+Nalo
Nalo+UCM924
F
G
Veh+CTOP
CTOP+UCM924
H
I
Veh+Nalt
Nalt+UCM924
n.s.

Figure 3. The non-selective naloxone and selective MOR antagonist CTOP block the effects of MT_2 on ON and OFF cells of the PAG-RVM descending antinociceptive pathway. (A) Schematic illustration of microinjections in the vlPAG site (left) and of site of the electrophysiological recording in the RVM (right). **(B)** Schematic illustration of the location of vlPAG and RVM microinjection sites. (Top) Vehicle or drug(s) microinjections were performed in the left vlPAG (filled blue circle). The open circle indicates microinjections accidentally or intentionally performed outside of vlPAG and were excluded from the analysis. (Bottom) Neuronal recordings were performed by lowering a glass electrode into the RVM. ON cells (red circles) or OFF cells (black circles) recording sites are shown. Some sites are not shown because of symbol overlapping. Distances from the bregma are indicated. (Top right). Representation of coronal sections of the rat brain with the photomicrograph of the recording site in the RVM. Raphe Magnus nucleus (RMg); raphe pallidus nucleus (RPa). The white arrow indicates the site of the electrode recording labeled with pontamine sky blue dye. (**C**) Firing rate histogram of a single ON (top left) and OFF (top right) neuron of the RVM after Veh followed by UCM924 microinjections, and of a single ON (bottom left) and OFF (bottom right) neuron of the RVM after naloxone followed by UCM924 microinjections. Scale bars indicate 5 minutes for ratemater records, and arrowheads indicate the noxious stimulation. UCM924 (10 μg, intra-vlPAG) decreases spontaneous firing rate activity of ON cells (**D, F, H**) and increases the firing activity of OFF cells (**E, G, I**) across time in neuropathic rats. Pretreatment with 1μg intra-vlPAG of naloxone (**D-E**) and CTOP (**F-G**), but not naltrindole (**H-I**), blocked the UCM924-induced modulation of ON (**D, F, H**) and of OFF cells (**E, G, I**). Data are expressed as mean ± SEM for n=4-2 each group (**D-I**). *P < 0.05, **P < 0.01, and ***P < 0.001 vs -5 min Veh+UCM924; ##P < 0.01, and ###P < 0.001 vs naloxone or CTOP + UCM924; $P< 0.05, $$P < 0.01, and $$$P < 0.001 vs -5 min Nalt+UCM924. Two-way ANOVA followed by Tukey post-hoc test.

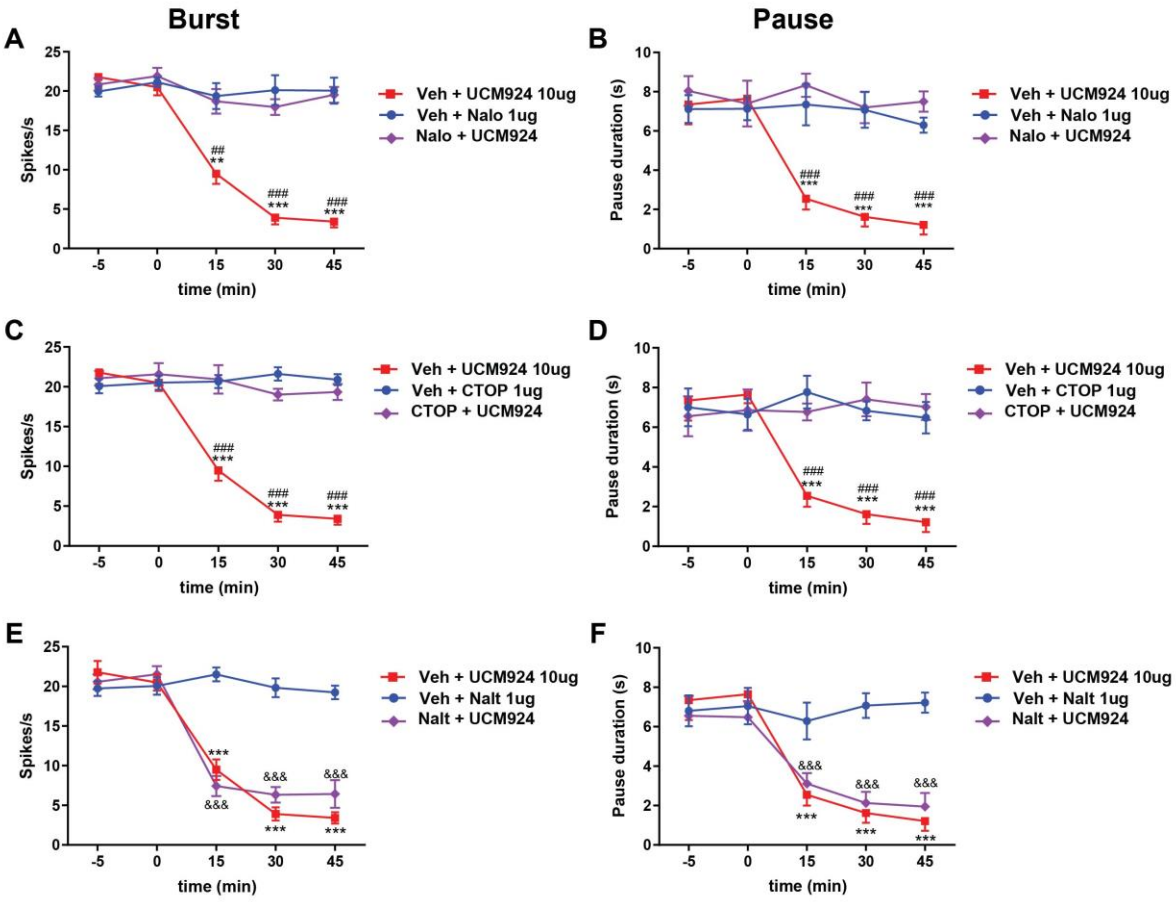

Figure 4. The non-selective naloxone and selective MOR antagonist CTOP block the effects of the MT_2 agonist UCM924 on ON cell burst and OFF cell pause of the PAG-RVM descending antinociceptive pathway. UCM924 (10 µg, intra-vlPAG) reduces the burst activity of ON cell burst (**A**, **C**, **E**) and the duration of OFF cell pause (**B**, **D**, **F**) across time in neuropathic rats. Pretreatment with 1 µg intra-vlPAG of naloxone (**A-B**) and CTOP (**C-D**), but not naltrindole (**E-F**), blocked the UCM924-induced modulation of ON cell burst (**A**, **C** and **E**) and of OFF cell pause (**B**, **D** and **F**). Data are expressed as mean ± SEM for n= 4-2 each group. *P < 0.05, **P < 0.01, and ***P < 0.001 vs -5 Veh+UCM924; #P < 0.05, ##P < 0.01, and ###P < 0.001 vs naloxone/CTOP/naltrindole + UCM924; &&&P < 0.001 vs -5 Nalt+UCM924. Two-way ANOVA followed by Tukey post-hoc test.

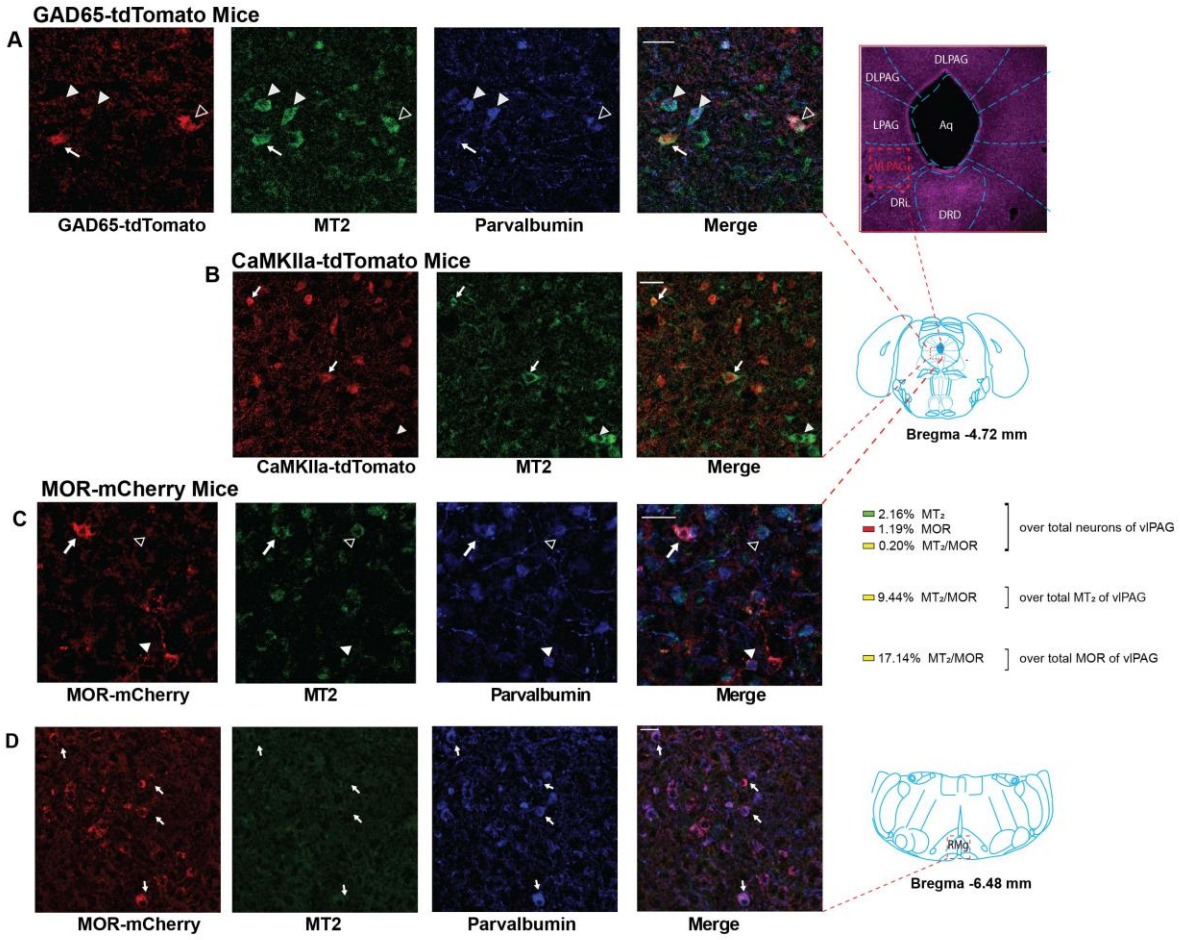

Figure 5. MT_2 receptor and MOR expression in the PAG-RVM descending pathway. (**A**) MT_2 receptors are expressed in GAD65-tdTomato$^+$ neurons of the vlPAG, and this colocalization was observed particularly in parvalbumin (PV) inhibitory expressing interneurons. (**B**) MT_2 receptors are expressed in CaMKIIα^+ neurons, an excitatory neuronal promoter of the adult forebrain. (**C**) MOR-mCherry, MT_2 receptor and inhibitory PV$^+$ GABAergic neurons are expressed in vlPAG. Both MOR-mCherry (filled arrowhead) and MT_2 (empty arrowhead) colocalize with PV$^+$ GABAergic neurons. Counting: 2.16 ± 0.32% of MT_2 receptor and 1.19 ± 0.18% of MOR-mCherry are expressed in the total neural cell body population of the vlPAG. Colabel MT_2^+/MOR-mCherry$^+$ neurons are 0.20 ± 0.02 % of the total neuronal population (arrow). **(D**) MT_2 receptors were not revealed in the RVM, while MORs are abundantly localized in this area. Scale bars: 25 μm.

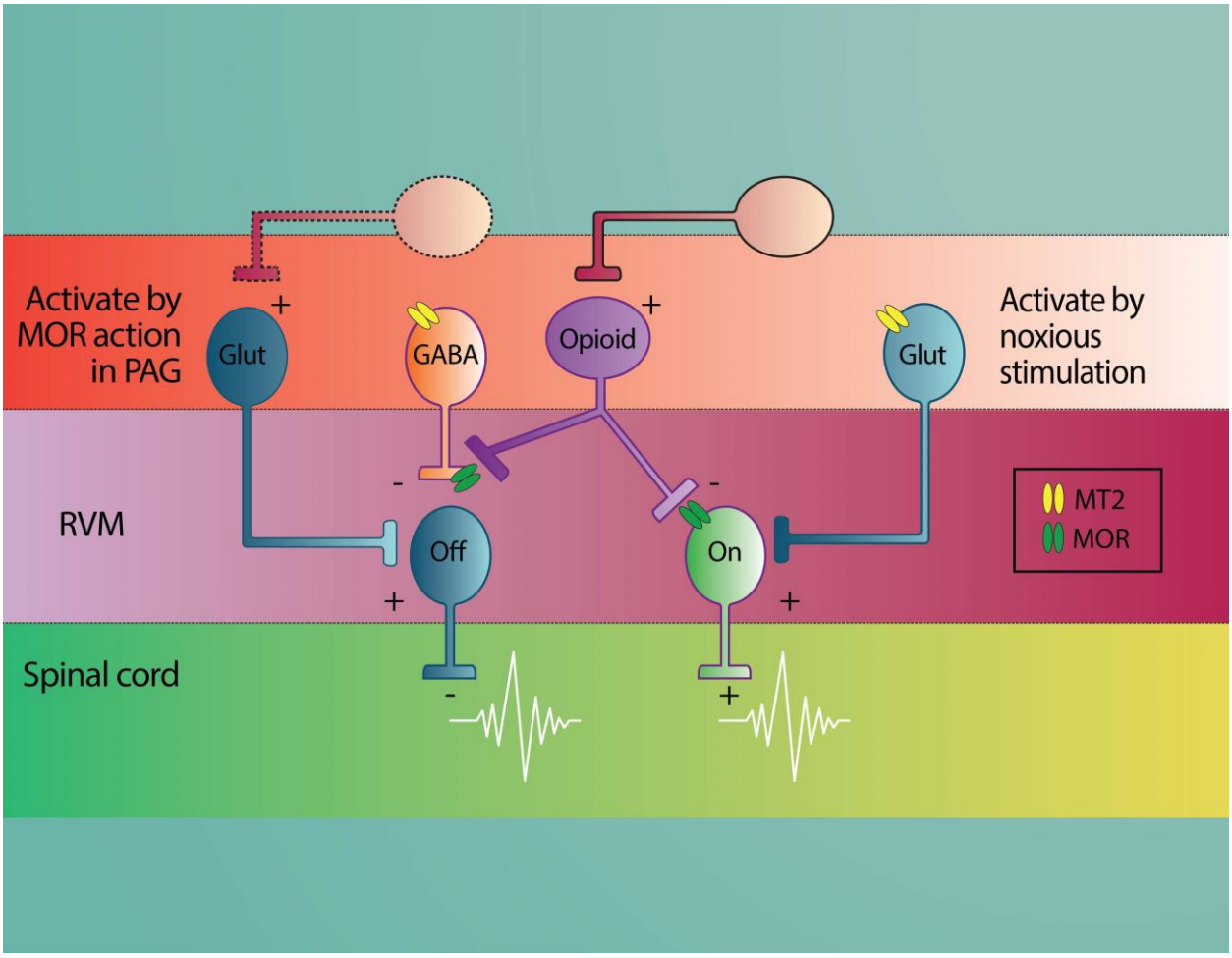

Figure 6. Schematic model to illustrating the role of MT_2 receptors and MORs in PAG-RVM circuit in nociceptive modulatory state. MT_2 receptors are located on both somatodendritic regions of GABA- and glutamatergic neurons in the vlPAG, but not in the RVM. The MT_2-mediated disinhibition of GABAergic projections positively modulates antinociceptive OFF, while MT_2 receptors silence glutamatergic inputs to pronociceptive ON cells in the RVM. MOR antagonism nullifies MT_2-induced anti-allodynia, confirming the upstream localization of MT_2 receptors in the pathway. MT_2: melatonin MT_2 receptor, MOR: μ-opioid receptor. Adapted with permission from Fields (2004)[30].